Photochemical Redox Reactions of Inner-Sphere Copper(II)-Dicarboxylate Complexes: Effects of the Dicarboxylate Ligand Structure on Copper(I) Quantum Yields

Lizhong Sun,[†] Chien-Hou Wu,*[,‡] and Bruce C. Faust[‡]

Duke University, School of the Environment and Department of Chemistry, Durham, North Carolina 27708-0328

Received: April 28, 1998

Studies were carried out on the photochemical redox reactions of a series of structurally related inner-sphere Cu(II)/dicarboxylate complexes in aqueous solution (N_2-purged), using steady-state illumination. Cu(I) quantum yields (313 nm) of these systems were characterized with respect to the effects of copper(II) speciation, mainly considering the effect of the dicarboxylate structure on the Cu(I) quantum yield. For each solution composition, which corresponds to a unique Cu(II) speciation, the Cu(II)-based molar absorptivity ($\epsilon_{Cu(II)}$, M^{-1} cm^{-1}) and the quantity $\Phi_{Cu(I)}\epsilon_{Cu(II)}$ (where $\Phi_{Cu(I)}$ represents the experimental Cu(I) quantum yield) were determined from experiments. This experimental information ($\epsilon_{Cu(II)}$ and $\Phi_{Cu(I)}\epsilon_{Cu(II)}$) was explicitly combined with the calculated equilibrium Cu(II) speciation (based on critically reviewed thermodynamic data) in a quantitative model to determine molar absorptivities (ϵ_{CuL}) and Cu(I) quantum yields ($\Phi_{Cu(I),CuL}$) of the CuL complexes, where L represents the dicarboxylate ligand. For Cu(dicarboxylate)^0, the observed relative reactivity of Cu(I) quantum yields at 313 nm ($\Phi_{Cu(I),CuL}$) varies by 50-fold and is affected by the dicarboxylate structure as follows: oxalate (0.42) > succinate (0.10) ≫ maleate (0.008). This trend in relative reactivity parallels the trend in expected relative stability of the carbon-centered radicals derived from decarboxylation of the carboxylate (i.e., acyloxyl) radicals formed in the initial photoinduced ligand-to-metal charge (electron) transfer reaction of the Cu(II)/dicarboxylate complex.

Introduction

Attention has been given to copper in marine and freshwater environments because of its biological requirement and because of its toxicity to phytoplankton and aqueous microorganisms.[1−8] The cellular uptake rate of copper and hence its toxicity to microorganisms are largely dependent on the chemical speciation of Cu(II) and specifically correlate best with $Cu(H_2O)_6^{2+}$, hereafter referred to as Cu^{2+}.[2−8] In seawater and freshwater, copper(II) is present as complexes with natural biogenic organic ligands,[3,4,7−11] which regulate the Cu^{2+} activity.[2−7,10,12]

Based on limited data, Cu(II) complexes of organic ligands are significantly photoreactive at terrestrial solar wavelengths > 290 nm.[13−15] Thus photochemical reactions of copper(II) complexes affect the redox cycling, and hence the speciation, of copper in natural waters.[4,5,10,15]

Conversely, the speciation of a transition metal also affects its photoreactivity.[16] Carboxylate (and phenolate) functional groups are abundant in natural organic ligands,[17] and it is thought that these functional groups are involved in the coordination of Cu(II) in natural waters. Thus, it is desirable to systematically study the photochemical reactions of Cu(II)/dicarboxylate complexes for a series of structurally related dicarboxylate ligands that represent a likely type of coordination environment experienced by organically bound Cu(II) in marine and freshwater environments.

To quantitatively characterize the photoproduction of Cu(I) from Cu(II) complexes it is necessary to minimize the confounding effects of rapid reoxidation of Cu(I) by O_2, $^{\bullet}O_2^-$, and HOOH.[14,18−20] Hence, it is necessary to study these reactions under O_2-free conditions.

The photoredox reactions of metal complexes proceed by the so-called ligand-to-metal charge (electron) transfer mechanism[14,15,21−25] and can be represented for Cu(dicarboxylate)^0 in O_2 free solutions by Scheme 1.[14,23,24] In Scheme 1, R represents a variable moiety in the dicarboxylate ligand: no R group for oxalate, CH_2 for malonate, CH_2CH_2 for succinate, and CH═CH for maleate. Photoexcitation of the Cu(dicarboxylate)^0 complex leads to an electronically excited state (denoted by a * in Scheme 1). As shown in Scheme 1, the excited state undergoes two major competing reactions: (1) return to the ground state by one or more mechanisms and (2) ligand-to-metal charge (electron) transfer from a carboxylate group ($-C(O)O^-$) to the Cu(II) center. For the Cu(maleate)^0 excited state, another possible competing pathway is isomerization to form Cu(fumarate)^0 (maleate, *cis*, fumarate, *trans*).

As shown in Scheme 1, upon electron transfer, a carboxylate radical (i.e., acyloxyl radical, carbonyloxyl radical) $^{\bullet}O(O)C-R-C(O)O^-$ and Cu(I) are formed together within the water solvent cage. The carboxylate radical within the water solvent cage with Cu(I), or as a free radical, undergoes two competing reactions. One, it decarboxylates producing CO_2 and a carbon-centered radical ($^{\bullet}R-C(O)O^-$).[14,21,24−36] And two, it receives back the electron from Cu(I) to reform the parent Cu(II) complex. This competition strongly affects the overall Cu(I) quantum yield, with decarboxylation favoring forward reaction and, hence, a higher Cu(I) quantum yield.

The photochemistry of Cu(II)/monocarboxylate complexes and the photoproduction of Cu(I) and CO_2 from Cu(II)/oxalate complexes have been studied.[5,14,25−27] Steady-state illumination

* To whom correspondence may be addressed: e-mail, chienhou@seas.ucla.edu.

[†] Current address: Komag Inc., 1704 Automation Parkway, San Jose, CA 95131.

[‡] University of California at Los Angeles, Department of Civil and Environmental Engineering, Environmental Chemistry Laboratory, 5731 Boelter Hall, Los Angeles, CA 90095-1593.

10.1021/jp982045g CCC: $15.00
Published on Web 10/13/1998

SCHEME 1

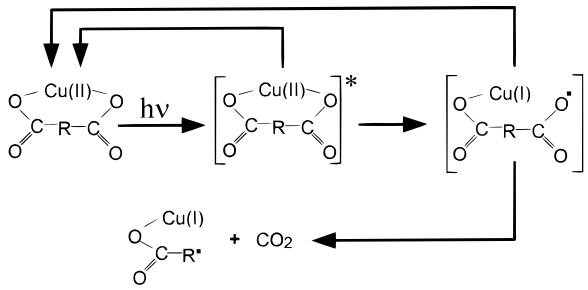

of Cu(II)/malonate complexes with 254-nm light, not present in terrestrial sunlight, causes decarboxylation of malonate and formation of CO_2.[23,24] A small photoproduction of Cu(I) from the Cu(II)/salicylate system was observed at 313 nm, although it could not necessarily be attributed to a photoinduced ligand-to-metal electron transfer.[5]

There have only been a few photochemical studies of Cu(II) complexes using solar wavelengths greater than 290 nm.[5,13−15] The dark (thermal) reduction of Np(VI)/dicarboxylate complexes to Np(V) has been reported.[28] But there has not been a thorough investigation of the effects of dicarboxylate ligand structure on the photoreactivity of a series of structurally related Cu(II)/dicarboxlate complexes in the solar wavelength region (> 290 nm).

For the above reasons, this study was initiated in order to (1) characterize the Cu(I) quantum yields and the molar absorptivities (absorption spectra) of the CuL complex of Cu^{2+} with a series of structurally related dicarboxylates and (2) further the understanding of the mechanisms of such photoreactions. Results will be reported here and in a future paper.

Theory

General Background. For each aqueous solution of a given Cu(II)/dicarboxylate system studied, the equilibrium speciation of copper(II), i.e., the equilibrium distribution of Cu(II) among its various complexes (species), is calculated by using critically reviewed thermodynamic equilibrium constants and a knowledge of the temperature and the solution composition: total initial concentration of Cu(II) ($[Cu(II)]_T$), total initial concentration of dicarboxylate ligand ($[L]_T$), total concentration of orthophosphate buffer, pH, and ionic strength. For a Cu(II) solution of a given dicarboxylate ligand, whose composition corresponds to a unique Cu(II) speciation, the Cu(II)-based molar absorptivity ($\epsilon_{Cu(II)}$, M^{-1} cm^{-1}) and the quantity $\Phi_{Cu(I)}\epsilon_{Cu(II)}$ (where $\Phi_{Cu(I)}$ is the experimental Cu(I) quantum yield) are determined independently from experiments. Each set of experimental information ($\epsilon_{Cu(II)}$ and $\Phi_{Cu(I)}\epsilon_{Cu(II)}$) is explicitly combined with the calculated equilibrium Cu(II) speciation in quantitative models (vide infra) to determine the molar absorptivity and Cu(I) quantum yield of each Cu(II) species,[37,38] with particular emphasis on the CuL complex in this study.

Molar Absorptivities of CuL (and of CuL_2 and Cu(HL)). At a given wavelength, the measured base-10 absorbance (A) of the Cu(II)/dicarboxylate solution can be expressed as[38]

$$A = D\{\epsilon_{CuL}[CuL] + \epsilon_{CuL_2}[CuL_2] + \epsilon_{Cu(HL)}[Cu(HL)] + \epsilon_{in}[Cu(II)]_{in} + \epsilon_L[L]_{free}\} \quad (1)$$

where D is the optical path length (cm), L denotes the completely deprotonated dicarboxylate^{2-} ligand, HL represents H(dicarboxylate)$^-$, the subscript "in" represents all forms of inorganic Cu(II), and the subscript "free" represents (dicarboxylate) ligand species that are not complexed with Cu(II). The various base-10 molar absorptivities (ϵ_i, M^{-1} cm^{-1}) are for individual species, excluding ϵ_{in}, which is an average (mean) value for all inorganic Cu(II) species (i.e., based on $[Cu(II)]_{in}$), and excluding ϵ_L, which is an average (mean) value for all free (dicarboxylate) ligand species (i.e., based on $[L]_{free}$). After rearranging eq 1, and by using $f_{CuL} \equiv [CuL]/[Cu(II)]_T$, $f_{CuL_2} \equiv [CuL_2]/[Cu(II)]_T$, $f_{Cu(HL)} \equiv [Cu(HL)]/[Cu(II)]_T$, and $f_{in} \equiv [Cu(II)]_{in}/[Cu(II)]_T$, where $[Cu(II)]_T \equiv [CuL] + [CuL_2] + [Cu(HL)] + [Cu(II)]_{in}$ (the initial total Cu(II) concentration), one obtains[38]

$$\epsilon_{Cu(II)} - \epsilon_{in}f_{in} = \epsilon_{CuL}f_{CuL} + \epsilon_{CuL_2}f_{CuL_2} + \epsilon_{Cu(HL)}f_{Cu(HL)} \quad (2)$$

where $\epsilon_{Cu(II)}$ is the experimental Cu(II)-based molar absorptivity (i.e., based on $[Cu(II)]_T$) and is defined as

$$\epsilon_{Cu(II)} \equiv (A/D - \epsilon_L[L]_{free})/[Cu(II)]_T \quad (3)$$

Equation 2 indicates that the difference of two measurable quantities, the Cu(II)-based molar absorptivity ($\epsilon_{Cu(II)}$) and the contribution from the inorganic copper(II) species ($\epsilon_{in}f_{in}$), is a linear combination of the weighted absorption of CuL, CuL_2, and Cu(HL), where the weighting of a Cu(II) complex is directly proportional to its relative molar abundance (f_{CuL}, f_{CuL_2}, and $f_{Cu(HL)}$).[38] The fundamental molar absorptivities of individual Cu(II) complexes (ϵ_{CuL}, ϵ_{CuL_2}, and $\epsilon_{Cu(HL)}$) are determined from a multivariate linear regression of eq 2.[38]

Cu(I) Quantum Yield of CuL (and CuL_2). For an aqueous Cu(II) solution with low total absorbance ($A \leq 0.12$) with measurable absorption by Cu(II) species and where the conversion of Cu(II) to Cu(I) is limited to < 10% of the initial total Cu(II) concentration, the initial rate of Cu(I) photoproduction ($R_{Cu(I)}^0$) can be expressed on an experimental basis as[38]

$$R_{Cu(I)}^0 = [\ln(10)]I_0\Phi_{Cu(I)}\epsilon_{Cu(II)}[Cu(II)]_T D \equiv j_{Cu(I)}[Cu(II)]_T \quad (4)$$

where I_0 is the volume-averaged incident light irradiance (einstein L^{-1} s^{-1}, 1 einstein = 1 mole of photons) and $\Phi_{Cu(I)}$ is the experimental Cu(I) quantum yield (mol $einstein^{-1}$). For a given aqueous Cu(II)/dicarboxylate solution, whose composition corresponds to a unique Cu(II) speciation, the quantity $\Phi_{Cu(I)}\epsilon_{Cu(II)}$ is determined from measurements of $R_{Cu(I)}^0$ and I_0 and from the known (controlled) values of $[Cu(II)]_T$ and D. The initial Cu(I) photoproduction rate $R_{Cu(I)}^0$ can also be expressed as the sum of the initial photoreaction rates of individual Cu(II) species:

$$R_{Cu(I)}^0 = [\ln(10)]I_0 D\{\Phi_{Cu(I),CuL}\epsilon_{CuL}[CuL] + \Phi_{Cu(I),CuL_2}\epsilon_{CuL_2}[CuL_2] + \Phi_{Cu(I),Cu(HL)}\epsilon_{Cu(HL)}[Cu(HL)] + \Phi_{Cu(I),in}\epsilon_{in}[Cu(II)]_{in}\} \quad (5)$$

where the various Cu(I) quantum yields (mole $einstein^{-1}$) are $\Phi_{Cu(I),CuL}$ for CuL, $\Phi_{Cu(I),CuL_2}$ for CuL_2, $\Phi_{Cu(I),Cu(HL)}$ for Cu(HL), and $\Phi_{Cu(I),in}$ for the average (mean) of all inorganic Cu(II) species. After equating eqs 4 and 5 and recalling that $f_{CuL} \equiv [CuL]/[Cu(II)]_T$, $f_{CuL_2} \equiv [CuL_2]/[Cu(II)]_T$, and $f_{Cu(HL)} \equiv [Cu(HL)]/[Cu(II)]_T$, one obtains

$$\Phi_{Cu(I)}\epsilon_{Cu(II)} - \Phi_{Cu(I),in}\epsilon_{in}f_{in} = \Phi_{Cu(I),CuL}\epsilon_{CuL}f_{CuL} + \Phi_{Cu(I),CuL_2}\epsilon_{CuL_2}f_{CuL_2} + \Phi_{Cu(I),Cu(HL)}\epsilon_{Cu(HL)}f_{Cu(HL)} \quad (6)$$

According to eq 6 the difference of the two measured quantities, $\Phi_{Cu(I)}\epsilon_{Cu(II)}$ and the corresponding contribution from inorganic Cu(II) species ($\Phi_{Cu(I),in}\epsilon_{in}f_{in}$), is a linear combination

TABLE 1: Composition Matrix for the Calculated Equilibrium Speciation of Cu(II): Cu(II) Species and Their Corresponding Components, Stoichiometric Coefficients, and Equilibrium Formation Constants[a,b]

species	components[c] Ox^{2-}	Su^{2-}	$Malea^{2-}$	Cu^{2+}	H^+	CO_3^{2-}	PO_4^{3-}	Cl^-	equilib const[a] $\log_{10}(\beta)$	notes[d]
$Cu(Ox)^0$	1			1					4.85	0.10, 25°
$Cu(HOx)^+$	1			1	1				6.32	0.10, 25°
$Cu(Ox)_2^{2-}$	2			1					8.85	0.10, 25°
$Cu(Su)^0$ [e]		1		1					2.70	0.10, 25°
$Cu(HSu)^+$		1		1	1				7.09	0.10, 25°
$Cu(Malea)^0$			1	1					3.41	0.10, 25°
$Cu(Malea)_2^{2-}$			2	1					5.20	0.10, 25°
$Cu(Malea)_3^{4-}$			3	1					6.20	0.20, 25°
$Cu(HPO_4)^0$				1	1		1		14.85	0.10, 25°
$Cu(H_2PO_4)^+$				1	2		1		19.83	0.15, 37°
$Cu(CO_3)^0$				1		1			5.88	→ 0, 25°
$Cu(CO_3)_2^{2-}$				1		2			9.32	→ 0, 25°
$Cu(HCO_3)^-$				1	1	1			11.25	→ 0, 25°
$Cu(OH)^+$				1	−1				−7.68	0.10, 25°
$Cu(OH)_2^0$				1	−2				−16.43	→ 0, 25°
$Cu(OH)_3^-$				1	−3				−26.87	1.0, 25°
$Cu(OH)_4^{2-}$				1	−4				−39.65	1.0, 25°
$Cu_2(OH)_2^{2+}$				2	−2				−10.72	1.0, 25°
$Cu_2(OH)^{3+}$				2	−1				−5.58	3.0, 25°
$Cu_3(OH)_4^{2+}$				3	−4				−21.54	0.10, 25°
$CuCl^+$				1				1	−0.04	→ 0, 25°
$Cu(Cl)_2^0$				1				2	−0.51	→ 0, 25°
$Cu(Cl)_3^-$				1				3	−2.95	→ 0, 25°
$Cu(Cl)_4^{2-}$				1				4	−5.03	→ 0, 25°

[a] All equilibrium constants reported here are for 25 °C (except where noted otherwise), 1.0 atm, and ionic strength $I = 0.10$ M. In certain cases equilibrium constants have been converted from a value for another ionic strength to a value for ionic strength = 0.10 M (as listed in this table), using the Davies equation.[43] [b] Equilibrium formation constants (β) and pK_a values are from critical reviews.[40−42] [species] = β[component 1]^i[component 2]^j[component 3]^k..., where [ ] signifies molar concentration of the species/component; *i*, *j*, *k*, ... are stoichiometric coefficients for the corresponding component (given in the matrix above), and β is the equilibrium formation constant of the species. Blank entries in the table are zero. The pK_a values of the species (25 °C, 1.0 atm., I = 0.10 M; original source, and as used here) are oxalic acid (1.1, 3.83), succinic acid (4.00, 5.24), maleic acid (1.75, 5.84), H_2CO_3* (6.13, 9.88) where $H_2CO_3^* \equiv H_2CO_3(aq) + CO_2(aq)$, and H_3PO_4 (1.92, 6.71, 11.65). For $K_w = [H^+][OH^-]$, $\log_{10}(K_w) = -13.78$ (25 °C, 1.0 atm, I = 0.10 M; original source, and as used here). [c] $Ox^{2-} \equiv$ oxalate^{2-}, $Su^{2-} \equiv$ succinate^{2-}, and $Malea^{2-} \equiv$ maleate^{2-}. HOx^- and HSu^- represent the monoprotonated forms of the dicarboxylate ligands. [d] Ionic strength (molar) and temperature (°C) of the original source of the thermodynamic data. [e] There is little evidence for the existence of Cu(succinate)$_2^{2-}$.[42] If a value of $\log_{10}(\beta) = 3.3$ (0.10 M ionic strength, 25 °C) for Cu(succinate)$_2^{2-}$ is used in speciation calculations, it has a small effect (<15% change) on the calculated equilibrium concentrations of Cu(II) species. See the Supporting Information for more information.

of the weighted individual contributions of $\Phi_{Cu(I),i}\epsilon_i$ for CuL, CuL_2, and Cu(HL), where the weighting is proportional to the relative molar fraction of each Cu(II) species f_i. Therefore, the fundamental photochemical quantity for CuL ($\Phi_{Cu(I),CuL}\epsilon_{CuL}$), as well as for CuL_2 ($\Phi_{Cu(I),CuL_2}\epsilon_{CuL_2}$) and Cu(HL) ($\Phi_{Cu(I),Cu(HL)}\epsilon_{Cu(HL)}$), is determined from multivariate linear regression of eq 6.[38]

General Considerations. Tris complexes (CuL_3) of Cu^{2+} with these dicarboxylate ligands are seldom reported[39−41] and are not expected due to the bidentate nature of the ligands and due to the Jahn−Teller elongation of the two axial Cu(II) coordinative bonds, effectively giving rise to square planar (D_{4h}) coordination geometry of the Cu(II) center. Through experimental design (1) values of f_{in} are normally small and the Cu(II) speciation is usually dominated by two species (e.g., CuL/CuL_2 or CuL/Cu(HL)) and/or (2) the contribution of inorganic Cu(II) to the observed absorbance or photochemistry is minor. In such cases the multivariate regressions (eqs 2 and 6) are limited to two independent variables, representing, for example, the species CuL/CuL_2 or CuL/Cu(HL). In addition to the Cu(II) speciation (f_{CuL}, f_{CuL_2}, $f_{Cu(HL)}$, f_{in}, etc. of eq 6), occasionally (but not for systems studied here) other factors influence the Cu(I) quantum yields independent of their effects on Cu(II) speciation: the absolute concentrations of free and complexed dicarboxylate and Cu(II) species and pH.[23,24,27]

With CuL as an example, the independently determined values of $\Phi_{Cu(I),CuL}\epsilon_{CuL}$ and ϵ_{CuL} are used to calculate the Cu(I) quantum yield for CuL ($\Phi_{Cu(I),CuL}$). Thus, based on this approach, the effect of dicarboxylate ligand structure on photoreactivity can be compared for complexes of the same stoichiometry (primarily CuL in this study).

Experimental Section

Equilibrium Speciation Calculations. The MINTEQA2 computer program[39] was used to calculate the equilibrium concentrations of all chemical species in each Cu(II)/dicarboxylate solution studied here: e.g., [CuL], [CuL_2], [Cu(HL)], $[Cu(II)]_{in}$, $[L]_{free}$, etc. Equilibrium constants and pK_a values that were used in these calculations are listed in Table 1 and are from critical reviews.[40−43] The water/ligand exchange reactions of Cu(II) are rapid,[44] excluding reactions with EDTA-type chelates (which were not studied here),[7] consistent with use of an equilibrium speciation model to describe the Cu(II) speciation.

Materials and Equipment. Glassware and quartzware were cleaned with a 50/50 v/v mixture of methanol (99.9%, Fisher, spectranalyzed) and aqueous 3.0 M HCl (Mallinckrodt) and thoroughly rinsed with Milli-Q water.[45] Unless otherwise noted, all reagents used in this study were reagent grade or HPLC grade and were used as received. All of the ligands were obtained from Fluka (heavy metal impurities <0.0005% m/m): oxalic acid, sodium salt (>99.5%); succinic acid (>99.5%); maleic acid (>99%). Other reagents used were $CuCl_2 \cdot H_2O$ (Alfa, 99.999%), NaH_2PO_4 (GFS, bio-refined; Cu, Fe, and Mn, 0.0005% m/m each), NaCl (Fisher; Fe and heavy metals, 0.5

ppm each), NaOH (Fisher; Cu and Fe, 0.0002% each; heavy metals (as Ag), 0.0004%), HCl (Fisher trace metal grade, Cu <0.5 ppbm, Fe <1 ppbm, Mn <0.1 ppbm), bathocuproine (sulfonated sodium salt, GFS), $(NH_2OH)_2 \cdot H_2SO_4$ (99.999%, Aldrich), CuCl (99.999% on a metals basis, Johnson Matthey), sodium acetate anhydrous (Mallinckrodt), glycolic acid (99%, Aldrich), 2-nitrobenzaldehyde (98%, Aldrich), CH_3CN (HPLC grade, Mallinckrodt or Fisher), and H_2SO_4 (heavy metals 0.0001%, Fe 0.00002%, GFS). Ultrahigh purity N_2 (99.9995%, Scott Specialty Gases) was used to purge solutions of bathocuproine, Cu(I), and Cu(II). All solutions were prepared by using only ultrahigh-purity Milli-Q water (≥18.2 MΩ cm resistivity). Solutions (or aliquots) were filtered through a 0.2-μm syringe filter (13 mm Teflon, or 25 mm Tuffryn; Acrodisc, Gelman). Gastight injection vials (40 mL, 28 × 95 mm, ≈22-mm Teflon-faced silicone septa, National Scientific Co.) were used to N_2-purge stock solutions of bathocuproine, Cu(I), and Cu(II).

Ultraviolet−visible absorbance measurements used a Varian Cary 3E UV/vis spectrophotometer and a custom-built constant-temperature (25 °C, Fisher 910 recirculator) variable-path-length aluminum cuvette holder (black-anodized). Absorbance measurements of Cu(II) solutions used Teflon-stoppered 10.00-cm quartz cuvettes (Starna). Photochemical experiments and chemical actinometry used gastight 100% fused-quartz cuvettes (5.00-cm path length, Spectrocell Inc.; R-3050-I; FUV; modified to 70 mm overall height) equipped with a 12-mm Teflon-faced silicone septum (Sun Brokers, 200594) and a Teflon screw cap. Single wavelength measurements (313 nm) were averaged over 120 s.

Solution Preparation and Absorption Spectra. Stock solutions of $CuCl_2 \cdot H_2O$ (in Milli-Q water), $[Cu(II)]_T \approx 0.010$ or 0.10 M, were prepared gravimetrically and filtered through a precleaned 0.2-μm filter. A given Cu(II)/dicarboxylate solution was prepared, with minimal/indirect room lighting, by adding an aliquot of the Cu(II) stock solution to a premade aqueous solution of total dicarboxylate ligand concentration ($[L]_T$), 100 μM total orthophosphate, and ionic strength = 0.10 M (NaCl, almost always 0.10 M). Adjustment of pH (with negligible dilution), used HCl (0.050 or 0.50 M) or freshly prepared 1.0 M NaOH, almost always after addition of Cu(II). Final pH measurements (±0.03) were made after adding and mixing all reagents on a separate aliquot of the solution that was not used for any other measurement.

Table 2 summarizes the solution conditions used for this study, which were optimized from the equilibrium speciation calculations. Typically, $[Cu(II)]_T$ and $[L]_T$ were held constant while the pH was varied, or pH and $[Cu(II)]_T$ were kept constant while $[L]_T$ was varied. The criteria of a minimum absorbance of ≈0.010 (at 313 nm) due solely to Cu(II) species almost always limited the lowest total Cu(II) concentration that could be used for photochemical experiments.

For spectral measurements of a given Cu(II)/dicarboxylate solution, (1) all solutions were filtered (0.2 μm), (2) 100 μM total orthophosphate and 0.10 M NaCl, at the desired pH, was used as the blank and reference, and (3) the contribution of $[L]_{free}$ to the absorbance (eq 3) was subtracted by including the dicarboxylate ligand ($[L]_T$) in the reference/blank solution or by using the calculated value of $[L]_{free}$ and the measured value of ϵ_L (determined from a solution without added Cu(II), but with otherwise identical composition). Values of ϵ_L (M^{-1} cm^{-1}) at 313 nm are dependent on pH and range from 0.01 to 0.19 for oxalate, 0.012 to 0.020 for succinate, and 0.9 to 10.6 for maleate.

TABLE 2: Composition of Cu(II)/Dicarboxylate Solutions[a]

dicaboxylate (L)	$[Cu(II)]_T$, μM	$[L]_T$, μM	pH
oxalate	10	450	3.50, 5.00
	25	190−270	7.00
	50	500	3.00−7.00
	500	1000	3.00−5.00
succinate	25	4900	4.50−6.50
	50	10000−50000	4.00−6.50
maleate	50	500	5.00−6.00
	25	6500, 7300	7.00
	50	500−2000	6.00

[a] All solutions were studied at 25 °C, contained 100 μM total orthophosphate to buffer the pH (±0.03), had an ionic strength of 0.10 M (adjusted with NaCl, almost always 0.10 M), and were filtered (0.2 μm). All solutions for photochemical experiments and Cu(I) measurements were N_2-purged. All solutions for spectral measurements were saturated with ambient laboratory air. Solutions did not contain any precipitates and were below the calculated solubility limit of all solids. $[Cu(II)]_T$ = total concentration of Cu(II). $[L]_T \equiv$ total concentration of dicarboxylate ligand. The exact composition of each solution studied is described in the Supporting Information.

Analytical Equipment and Measurements. Solution pH was measured with an Orion Model SA 720 pH meter, combination glass electrode (Orion 8103 Ross), and NIST-traceable standard buffers (Fisher): 5.00 (potassium biphthalate buffer) and 6.00, 7.00, 7.40, and 8.00 (all orthophosphate buffers).

Copper(I) was quantified by using the bathocuproine method[46,47] and the literature value of the Cu(I)-based molar absorptivity at 484 nm of 1.24×10^4 M^{-1} cm^{-1} (which agreed within 3% of that determined as a check in this study).[47] The absorbance (484 nm) of 1 μM Cu(I) (100 μM bathocuproine) was negligibly affected (<6%) by each dicarboxylate at the highest concentration studied. Copper(I) was measured directly in the gastight cuvette without transfer. Within 30 s of interupting illumination (under red lighting), 100 μL of a continuously N_2-purged (>90 min) bathocuproine solution was withdrawn with a syringe and immediately injected into the solution containing Cu(I) (giving $[bathocuproine]_T = 100$ μM). After mixing 1−10 min in the dark, the constant absorbance was measured by averaging over 120 s or by averaging 10 sequential readings.

N_2 Purging. N_2 purging was used to remove O_2 from solutions [of Cu(II)/dicarboxylate, bathocuproine, Cu(I), and Cu(II)] to ensure an accurate measurement of Cu(I). A given Cu(II)/dicarboxylate solution was purged in a gastight quartz cuvette (vide supra) with ultrahigh purity N_2 (equipped with an O_2 trap, Oxiclear DGP-250-R1, Labclear) while mixing with a Teflon-coated magnetic stir bar. The N_2 gas was delivered (0.020 L min^{-1}; Scott rotameter; stainless steel metering valve M2T1, Dakoda Instr.) through a Teflon "syringe needle" (20-gauge, Aldrich) through the Teflon-faced silicone septum: (1) to the bottom of the cuvette for >90 min prior to illumination and (2) kept above the surface of the solution during illumination (≤90 min).

The stability of Cu(I) during such procedures was tested as follows. Milli-Q water (20.0 mL) in a 5.00-cm gastight (septum) quartz cuvette was stirred and purged for 90 min with N_2, after which 15.0 μL of aqueous 5.0 mM CuCl solution (in 0.10 M HCl and 1.0 M NaCl), which was N_2-purged by the same procedure, was injected into the cuvette with a syringe. After mixing for a given time (30 s or 90 min), an aliquot of a continuously N_2-purged (>90 min) bathocuproine solution, was injected into the well-mixed solution with a syringe (giving $[bathocuproine]_T = 100$ μM). The difference in absorbance

(484 nm) between the two solutions (30 s, 90 min) was small (<2%). Moreover, addition of 1% hydroxylamine, to rapidly reduce any Cu(II) to Cu(I),[47] had negligible effect (<3%) on the absorbance (484 nm). Thus, the N_2-purging procedure used here minimized oxidation of Cu(I) by O_2 and/or by O_2-derived oxidants for the time scales (≤90 min) of these experiments.

General Photochemical Procedures. Steady-state illuminations (25 °C, 313 nm) used a 1000-W O_3-free Hg−Xe lamp, a monochromator (entrance and exit slits = 2.5 mm; full bandwidth at half-peak-height ≈ 7−8 nm; Spectral Energy Corp., Kratos, Schoeffel),[45] two 2.5-mm Hoya UV-30 optical glass filters to filter light exiting the monochromator, and 20.0 mL of solution (Cu(II)/dicarboxylate or chemical actinometer). For Cu(II) (photo)reactions, each kinetic data point corresponded to a separate fresh aliquot of a N_2-purged Cu(II)/dicarboxylate solution that was reacted for a known time.

Thermal (dark) formation of Cu(I) was characterized for each photochemical experiment, using an aliquot of the same N_2-purged solution that was kept in the dark. The minor contribution of Cu(I) photoproduction from inorganic Cu(II) was determined for a solution without added dicarboxylate ligand but with otherwise identical composition as the Cu(II)/dicarboxylate solution.

Values of I_0 (einstein L^{-1} s^{-1}) at 313 nm were determined by chemical actinometry (20.0 mL of an air-saturated aqueous solution of 4.0 μM 2-nitrobenzaldehyde), and the quantity $\Phi_{313}\epsilon_{313} = 640 \pm 44$ L einstein^{-1} cm^{-1} as described previously[45] ($r^2 \geq 0.99$ for linear regressions of all first-order kinetic plots). Measured experimental values of I_0 at 313 nm ranged from 0.44 to 1.33 μ(einstein) L^{-1} s^{-1}, and values of I_0L ranged from 2.2 to 6.7 n(einstein) cm^{-2} s^{-1}.

Calculated Photoreaction Rate Constants of Cu(II)/Dicarboxylate Complexes in Sunlight. The apparent first-order rate constant for direct photoproduction of Cu(I) from a given Cu(II)/dicarboxylate complex (CuL and CuL_2) in terrestrial sunlight ($j_{i\rightarrow Cu(I)}$) was estimated by using (1) the measured absorption spectra (ϵ_i for wavelengths 290−340 nm, data not shown here), (2) wavelength-dependent values of $\Phi_{Cu(I),i}$ that were based on values for 313 nm reported here and assuming $\Phi_{Cu(I),i}(\lambda) = \Phi_{Cu(I),i}(313)$ for $\lambda \leq 313$ nm and $\Phi_{Cu(I),i}(\lambda) = \Phi_{Cu(I),i}(313)[\epsilon_i(\lambda)/\epsilon_i(313)]$ for $313 < \lambda \leq 340$ nm, (3) published spherically integrated solar irradiance values for a solar zenith angle of 30°,[48] and (4) equations and procedures described previously.[49]

Results and Discussion

Copper(II) Speciation. For each Cu(II)/dicarboxylate system studied, the equilibrium Cu(II) speciation (25 °C) was calculated by using equilibrium constants given in Table 1 and the known solution composition ($[Cu(II)]_T$, $[L]_T$, pH (100 μM total orthophosphate), and 0.10 M ionic strength (NaCl, nearly always 0.10 M)). From equilibrium speciation calculations for the conditions of the photochemical experiments, the complexes CuL, CuL_2, and Cu(HL) represented cumulatively the following percentage of the total Cu(II) species [$100(f_{CuL} + f_{CuL_2} + f_{Cu(HL)})$]: ≥93% for Cu(II)/oxalate (for all but one experiment), ≥52% for Cu(II)/succinate (for all but two experiments), and ≥71% for Cu(II)/maleate (for all but two experiments). For the 313-nm spectral measurements made at pH < 7.00, the complexes CuL, CuL_2, and Cu(HL) represented cumulatively the following percentages of the total Cu(II) species [$100(f_{CuL} + f_{CuL_2} + f_{Cu(HL)})$]: ≥83% for oxalate, ≥71% for succinate, and 10−94% for maleate. For the conditions of this study inorganic Cu(II) represented a significant fraction of the total Cu(II); however, inorganic Cu(II) was a comparatively weak absorber and photolyzed much less efficiently than the least reactive Cu(II)/dicarboxylate complex studied here [$\Phi_{Cu(I),in}\epsilon_{in}$ (L einstein^{-1} cm^{-1}) at 313 nm = 0.084 at pH = 7.00 and 0.020 at pH = 5.27].

Controls. Results of controls show that the rate of Cu(I) production from thermal (dark) reactions of the Cu(II)/dicarboxylate solution is ≤4% of the Cu(I) photoformation rate. In any case, for each kinetic data point the small concentration of thermally (dark) formed Cu(I) was subtracted from the measured total Cu(I) concentration formed in the photolyzed solution, to determine the concentration of photoformed Cu(I).

It was also useful to test for indirect formation of Cu(I), from thermal reactions of Cu(II) with (meta)stable photoproducts derived from direct photoreaction of the free dicarboxylate species [i.e., not complexed with Cu(II)]. For this control, a N_2-purged solution of the dicarboxylate ligand, with a chemical composition identical to that of the Cu(II)/dicarboxylate solution but without added Cu(II), was illuminated for the same amount of time as was the corresponding Cu(II)/dicarboxylate solution. Immediately after stopping illumination, an amount of Cu(II) close to the amount of Cu(I) formed in the similarly illuminated Cu(II)/dicarboxylate solution was injected (as a N_2-purged Cu(II) solution) into the photolyzed dicarboxylate solution. The solution was mixed for 10−20 min in the dark, after which Cu(I) was quantified. As determined by this procedure, indirect Cu(I) photoproduction represented <3% of the Cu(I) formed during photoreaction of the Cu(II)/dicarboxylate solution, for each Cu(II)/dicarboxylate system studied. Copper(I) quantum yields were not affected by the presence or absence of 100 μM total orthophosphate buffer, for solutions with otherwise identical composition.

Molar Absorptivities of Individual Cu(II) Complexes. The total absorbance of a given Cu(II)/dicarboxylate solution was corrected for the absorbance by the uncomplexed forms of the dicarboxylate ligand itself, as described in the Experimental Section. This correction was normally small (<4% at 313 nm), except in the case of Cu(II)/maleate, where uncomplexed maleate species themselves contributed 40−86% of the total absorbance at 313 nm. For the conditions of this study inorganic Cu(II) contributed the following percentage of the total absorbance of all Cu(II) species: ≤6% for oxalate, ≤20% for succinate, and 50−90% for maleate.

Equation 2 predicts a linear relationship between the quantity ($\epsilon_{Cu(II)} - \epsilon_{in}f_{in}$) and the calculated equilibrium fractions of CuL (f_{CuL}), CuL_2 (f_{CuL_2}), and Cu(HL) ($f_{Cu(HL)}$). Multivariate linear regression analysis (intercept forced through zero) of eq 2 was used to determine values of ϵ_{CuL}, ϵ_{CuL_2}, and $\epsilon_{Cu(HL)}$. Based on the linear-regression best-fit parameters (ϵ_{CuL}, ϵ_{CuL_2}, and $\epsilon_{Cu(HL)}$), on the independently calculated equilibrium Cu(II) speciation (f_i), and on other known or measured experimental parameters (A/D, $\epsilon_L[L]_{free}$, $[Cu(II)]_T$, pH), values of $\epsilon_{Cu(II)} - \epsilon_{in}f_{in}$ that are calculated agree well with measured values of $\epsilon_{Cu(II)} - \epsilon_{in}f_{in}$: Cu(II)/oxalate (<12% difference), Cu(II)/succinate (<10% difference), and Cu(II)/maleate (<18% difference). As an example, Figure 1 illustrates the quality of fit of eq 2, which was used to determine the molar absorptivities for the Cu(II)/succinate system. Additional information about this procedure and about the quality of fits is available in the Supporting Information.

Table 3 shows the values of molar absorptivities of individual complexes (CuL and CuL_2) at 313 nm for each Cu(II)/dicarboxylate system studied here. The molar absorptivities for individual complexes at other wavelengths were determined in the same way (data not shown).

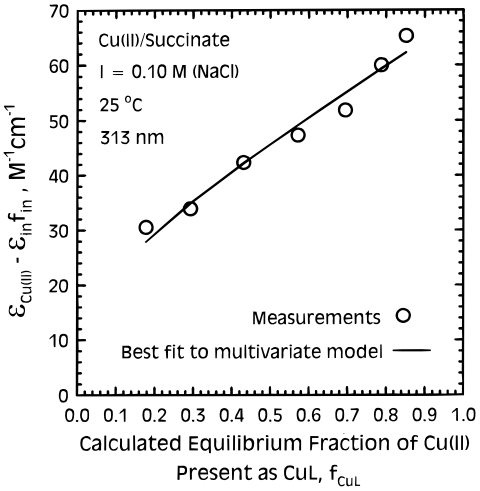

Figure 1. Comparison of the molar absorptivities for Cu(II)/succinate that were measured and the best-fit values (multivariate linear regression) determined from eq 2. Due to the nature of multivariate linear regression, the best-fit line shown here is not a continuous function in two dimensions.

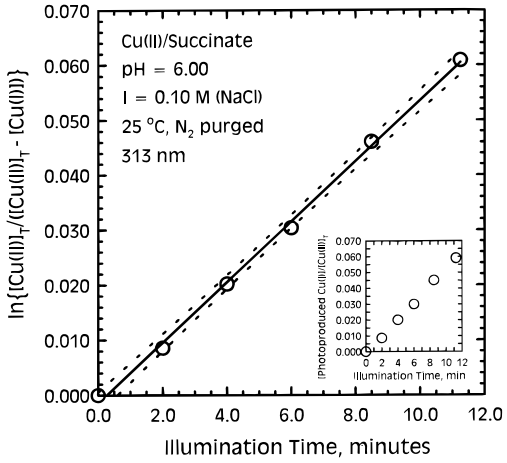

Figure 2. Kinetic behavior of Cu(I) photoproduction in the Cu(II)/succinate system at 313 nm (25 °C): $[Cu(II)]_T = 25\ \mu M$, $[L]_T = 4900\ \mu M$ total succinate, pH = 6.00 (100 μM total orthophosphate), and 0.10 M NaCl (ionic strength = 0.10 M). The slope of this plot (after correction for minor Cu(I) production in the dark) gives the apparent first-order photoreaction rate constant for Cu(I) photoproduction, $j_{Cu(I)}$ (eq 4). The dashed lines indicate the 95% confidence interval. Inset: raw kinetic data. For all of the Cu(II)/dicarboxylate systems studied, linear regression r^2 values for first-order kinetic plots of this type were ≥ 0.98 for all but one experiment.

Kinetics of Cu(I) Photoproduction from Cu(II)/Dicarboxylates. As an example, Figure 2 shows the kinetic plot of Cu(I) photoproduction (313 nm) for a Cu(II)/succinate solution. As expected from eq 4 and as shown in Figure 2, Cu(I) photoproduction follows first-order kinetics that is characterized by an apparent first-order rate constant (s^{-1}) for Cu(I) photoproduction ($j_{Cu(I)}$, as implicitly defined in eq 4). The initial rate of Cu(I) photoproduction, $R_{Cu(I)}{}^0$, is then determined by

$$R_{Cu(I)}{}^0 = j_{Cu(I)}[Cu(II)]_T \qquad (7)$$

Using the initial rate minimizes the potential influence of any possible back reactions of Cu(I), such as direct photoreaction of $CuCl_x^{1-x}$ [50] and oxidation by trace amounts of unremoved O_2, and minimizes any possible minor changes in the Cu(II) speciation during the photoreaction.

Copper(I) Quantum Yield of CuL ($\Phi_{Cu(I),CuL}$). For each solution of a given Cu(II)/dicarboxylate system studied, the quantity ($\Phi_{Cu(I)}\epsilon_{Cu(II)} - \Phi_{Cu(I),in}\epsilon_{in}f_{in}$) was determined for the conditions described in Table 2. Equation 6 predicts a linear relationship between the measured quantity ($\Phi_{Cu(I)}\epsilon_{Cu(II)} - \Phi_{Cu(I),in}\epsilon_{in}f_{in}$) and the calculated equilibrium molar fractions of CuL, CuL_2, and Cu(HL) (f_{CuL}, f_{CuL_2}, and $f_{Cu(HL)}$, respectively). Multivariate linear regression analysis (intercept forced through zero) of eq 6 was used to determine values of $\Phi_{Cu(I),CuL}\epsilon_{CuL}$ and for some dicarboxylates also values of $\Phi_{Cu(I),CuL_2}\epsilon_{CuL_2}$ or $\Phi_{Cu(I),Cu(HL)}\epsilon_{Cu(HL)}$. Based on the linear-regression best-fit parameters, on the independently calculated equilibrium Cu(II) speciation (f_i), and on other known or measured experimental parameters ($R_{Cu(I)}{}^0$, $[Cu(II)]_T$, etc.), values of the quantity $\Phi_{Cu(I),CuL}\epsilon_{CuL} - \Phi_{Cu(I),in}\epsilon_{in}f_{in}$ that are calculated agree well with measured values of the same quantity: Cu(II)/oxalate (<9%), Cu(II)/succinate (<41%), Cu(II)/maleate (<7%). As an example, Figure 3 illustrates the quality of fit of eq 6, which was used to determine the values of $\Phi_{Cu(I),CuL}\epsilon_{CuL}$ etc. for the Cu(II)/succinate system. Additional information about this procedure and the quality of fits is available in the Supporting Information.

Values of $\Phi_{Cu(I),CuL}\epsilon_{CuL}$ etc. determined by these procedures, and hence values of $\Phi_{Cu(I),CuL}$ etc. derived therefrom, are intended to be independent of the dicarboxylate concentration and speciation. Cu(I) quantum yields at 313 nm for CuL ($\Phi_{Cu(I),CuL}$) of the different Cu(II)/carboxylate complexes were determined by these procedures and are listed in Table 3. Due to reactions of H_2L/HL^- malonate species with $[Cu^I(^-O(O)C-R^\bullet)]^0$ formed during illumination of Cu(II)/malonate solutions,[23,24] Cu(I) photoformation is limited (by a mechanism not significant for systems studied here), and therefore, a more detailed kinetic model was used to determine values of $\Phi_{Cu(I),CuL}\epsilon_{CuL}$ for this system. Thus the results of the Cu(II)/malonate system will be described in a future paper.

Sensitivity Analyses. Values of $\Phi_{Cu(I),i}$ are determined from the quantities $\Phi_{Cu(I),i}\epsilon_i$ and ϵ_i, as described earlier. Sensitivity analyses were performed to determine the effect of the uncertainty in calculated equilibrium Cu(II) speciation (i.e., f_{CuL}, f_{CuL_2}, $f_{Cu(HL)}$, f_{in}, etc.), which is based on equilibrium constants and pK_a values given in Table 1 and on the experimental results reported here (Supporting Information). For all of these analyses the uncertainty in equilibrium formation constants of CuL and CuL_2 (or CuL and Cu(HL) for ϵ_i in the Cu(II)/succinate system) exhibited the greatest effect on the associated uncertainty in values of ϵ_i and $\Phi_{Cu(I),i}$.

Hence, for each Cu(II)/dicarboxylate system, sensitivity calculations were carried out, for which the equilibrium constants for CuL (β_{CuL}) and CuL_2 (β_{CuL_2}) were varied over a 4-fold range (increased or decreased by a factor of 2.0 relative to the best values of β_{CuL} and β_{CuL_2} given in Table 1). For each Cu(II)/dicarboxylate system, results of these calculations (four permutations) are summarized as ranges of the relevant parameters.

Ranges of ϵ_i ($M^{-1}\ cm^{-1}$) are 72−96 for Cu(oxalate)^0, 70−78 for Cu(oxalate)$_2^{2-}$, 63−87 for Cu(succinate)^0, and 59−144 for Cu(maleate)^0. Ranges of $\Phi_{Cu(I),i}$ (mol einstein^{-1}) are 0.40−0.44 for Cu(oxalate)^0, 0.41−0.43 for Cu(oxalate)$_2^{2-}$, 0.094−0.11 for Cu(succinate)^0, and 0.007−0.009 for Cu(maleate)^0. Since most of the published values of β_{CuL} and β_{CuL_2} are within a factor of ± 2.0 of the best values cited in Table 1, the above uncertainties are considered small.

Effect of Dicarboxylate Structure on the Cu(I) Quantum Yield and a Proposed Reaction Pathway. The Cu(I) quantum yields listed in Table 3 vary by 50-fold for the different Cu(II)/dicarboxylate complexes studied here. For example, the Cu(I)

TABLE 3: Summary of Molar Absorptivities (ϵ_{CuL} and ϵ_{CuL_2}, M^{-1} cm^{-1}) and Cu(I) Quantum Yields ($\Phi_{Cu(I),CuL}$ and $\Phi_{Cu(I),CuL_2}$, mole einstein^{-1}) for the Individual Complexes [Cu(dicarboxylate)^0 (CuL) and Cu(dicarboxylate)$_2^{2-}$ (CuL_2)], at 313 nm[a]

dicarboxylate	structure	ϵ_{CuL}	ϵ_{CuL_2}	$\Phi_{Cu(I),CuL}$	$\Phi_{Cu(I),CuL_2}$	$(\Phi_{Cu(I),CuL})(\epsilon_{CuL})$	$(\Phi_{Cu(I),CuL_2})(\epsilon_{CuL_2})$
oxalate	$^-O(O)CC(O)O^-$	82 ± 23	74 ± 16	0.42 ± 0.14	0.43 ± 0.10	35 ± 6	32 ± 4
succinate[b]	$^-O(O)CCH_2CH_2C(O)O^-$	70 ± 5		0.10 ± 0.02		7.1 ± 1.1	
maleate[c]	$^-O(O)CC(H)=C(H)C(O)O^-$	90 ± 17		0.008 ± 0.002		0.73 ± 0.02	

[a] Best value ± 1 standard deviation for 25 °C and 0.10 M ionic strength (NaCl). Solutions were purged with ultrahigh-purity N_2 for the Cu(I) quantum yield determinations. The range of solution compositions used to determine these values is given in Table 2 and in the Supporting Information. [b] $\epsilon_{Cu(HL)} = 29 \pm 9$ M^{-1} cm^{-1} (mean ± standard deviation). $(\Phi_{Cu(I),Cu(HL)})(\epsilon_{Cu(HL)}) \ll (\Phi_{Cu(I),CuL})(\epsilon_{CuL})$. [c] $(\Phi_{Cu(I),CuL_2})(\epsilon_{CuL_2}) \ll (\Phi_{Cu(I),CuL})(\epsilon_{CuL})$.

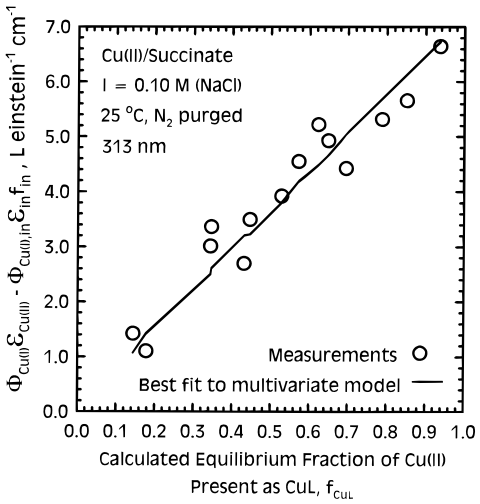

Figure 3. Comparison of the photochemical parameters for Cu(II)/succinate that were measured and the best fit values (multivariate linear regression) determined from eq 6. Due to the nature of multivariate linear regression, the best-fit line shown here is not a continuous function in two dimensions.

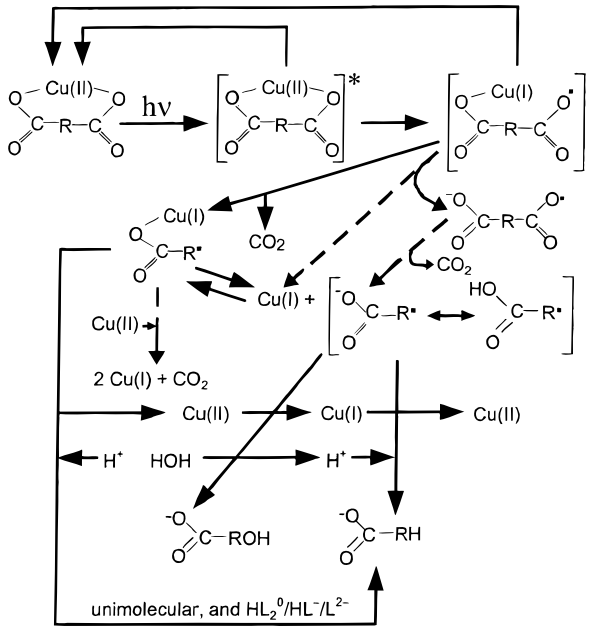

Figure 4. Proposed reaction scheme for photoreaction of Cu(II)/dicarboxylate complexes: no R group for oxalate, R is CH_2 for malonate, R is CH_2CH_2 for succinate, and R is C(H)=C(H) for maleate.

quantum yield for CuL is 0.42 for Cu(oxalate)^0, 0.15 for Cu(malonate)^0 (C. Wu and B. C. Faust, personal communication), 0.10 for Cu(succinate)^0, and only 0.008 for Cu(maleate)^0. A question, which derives from the results, is why do Cu(II) complexes of a series of structurally related dicarboxylate ligands exhibit so much difference in their Cu(I) quantum yields?

Based on the results of this study and on the literature,[14,23,24,27] the photoredox process of Cu(II)/dicarboxylates studied here is depicted in Figure 4.

For conditions of these studies the dicarboxylates and Cu^{2+} primarily form inner-sphere complexes of the type CuL, CuL_2, and (for succinate) Cu(HL). Each Cu(II) complex undergoes photoexcitation to form an electronically excited state (denoted by * in Figure 4); for simplicity, parallel photoreaction pathways of CuL_2 and Cu(HL) are not shown. The excited-state undergoes two competing reactions: (1) it is deactivated, with no net reaction and (2) it undergoes ligand-to-metal charge (electron) transfer, forming Cu(I) and a carboxylate radical (i.e., an acyloxyl radical, a carbonyloxyl radical) within the water solvent cage.

As shown in Figure 4, the carboxylate radical, either free or within the water solvent cage together with Cu(I), undergoes two major competing reactions that affect the Cu(I) quantum yield: (1) it receives back the electron from Cu(I), reforming the parent Cu(II)/dicarboxylate complex, or (2) it decarboxylates,[27,29−36] even within the water solvent cage, giving CO_2 and a Cu(I)/carbon-centered radical pair [$Cu^I(^-O(O)C-R^\bullet)$]^0. Competition between these two pathways strongly affects the overall Cu(I) quantum yield, and decarboxylation favors forward reaction and, hence, a higher Cu(I) quantum yield.

The rate of decarboxylation of the parent carboxylate radical is strongly affected by the stability of the carbon-centered radical formed as product. Since decarboxylation of the carboxylate radical (which increases the Cu(I) quantum yield) competes with recombination of the carboxylate radical with Cu(I) (no net reaction), the stability of the carbon-centered radical is expected to affect the overall Cu(I) quantum yield.

The carbon-centered radicals derived from decarboxylation of carboxylate radicals of the dicarboxylate ligands used in the study have different degrees of resonance stability, which are expected to follow the trend:

$$\text{oxalate} > \text{malonate} > \text{succinate} \gg \text{maleate}$$

The $^\bullet C(O)O^-$ radical, which is derived from decarboxylation of the oxalate radical, is expected to be comparatively easy to form, due to its resonance stabilization. In contrast, the carbon-centered radical derived from decarboxylation of the maleate carboxylate radical is comparatively difficult to form (unstable), because it is a vinyl radical ($-C(H)=C^\bullet$) which is not stabilized by resonance. On the basis of this relative stability sequence and on the knowledge that carboxylate radicals decarboxylate faster if they form stable carbon-centered radicals,[32] it is expected that the rate of decarboxylation of carboxylate radicals should follow the trend as listed above and that this should similarly affect the trend in Cu(I) quantum yields of the Cu(II)/dicarboxylate complexes, since decarboxylation competes with recombination. Consistent with this picture, the Cu(I) quantum yields of the Cu(II)/dicarboxylate systems follow the same trend as described above.

Additionally various reactions of the carbon-centered radical, either free or coordinated to Cu(I), influence the Cu(I) quantum

yield. These reaction pathways are shown in Figure 4 and are consistent with published reports, as described below for each dicarboxylate system. The relative importance of these various possible reaction pathways also depends on the dicarboxylate structure.

As shown in Figure 4, at least two competitve reactions of $[Cu^{I}(^{-}O(O)C-R^{\bullet})]^{0}$ affect the Cu(I) quantum yield: one, separation from the water solvent cage as Cu(I) and a free carbon-centered radical ($^{\bullet}R-C(O)O^{-}$); and, two back electron transfer from Cu(I) to the carbon-centered radical (unimolecular and mediated by free dicarboxylate ligand species[24]), reforming Cu(II) (i.e., no net Cu(I) photoproduction) and giving the corresponding carbanion, which reacts rapidly with H^{+} (and/or with H_2O, with loss of OH^{-}) to give a reduced organic photoproduct (R(H)-$C(O)O^{-}$).

By analogy, at least two competing reactions of the free carbon-centered radical ($^{\bullet}R-C(O)O^{-}$) influence the Cu(I) quantum yield.[51] In one, $^{\bullet}R-C(O)O^{-}$ accepts an electron from Cu(I), reforming Cu(II) (no net Cu(I) photoformation) and giving R(H)-$C(O)O^{-}$. In the other, $^{\bullet}R-C(O)O^{-}$ donates an electron to Cu(II), forming Cu(I) and R(OH)-$C(O)O^{-}$. Additionally, reduction of Cu(II) by $^{\bullet}R-C(O)O^{-}$ reportedly gives the corresponding alcohol and CO_2 as products [$^{\bullet}R-C(O)O^{-}$ + Cu(II) + $H_2O \rightarrow$ R(H)-OH + Cu(I) + CO_2].[20]

For the Cu(II)/oxalate system, the intermediate $[Cu^{I}(CO_2^{-\bullet})]^{0}$ was identified in flash photolysis experiments ($\lambda > 200$ nm),[27] consistent with the reaction scheme depicted in Figure 4. An apparent first-order rate constant (k_{obs}) for decay of $[Cu^{I}(CO_2^{-\bullet})]^{0}$ by reaction with Cu(II) was calculated by using eq I of ref 27 and was found to vary by a factor of 1790 for the conditions of our experiments. But the products of the decay of $[Cu^{I}(CO_2^{-\bullet})]^{0}$, Cu(I)/Cu(II) and $CO_2/HC(O)O^{-}$, were not experimentally identified and quantified,[27] so the effect of variable decay rate constants on measured values of $\Phi_{Cu(I)}\epsilon_{Cu(II)} - \Phi_{Cu(I),in}\epsilon_{in}f_{in}$ is not known. Measured values of $\Phi_{Cu(I)}\epsilon_{Cu(II)} - \Phi_{Cu(I),in}\epsilon_{in}f_{in}$ at 313 nm vary by <25% for a wide range of experimental conditions for all of the Cu(II)/oxalate experiments in this study (Supporting Information), including a 5-fold variation in $[Cu(II)]_T$ (at constant pH and nearly identical Cu(II) speciation), and are successfully quantified by eq 6. This indicates that variable decay rates for reaction of $[Cu^{I}(CO_2^{-\bullet})]^{0}$ with Cu(II) have negligible influence on the Cu(I) quantum yields (313 nm) for the conditions of experiments reported here.

From Figure 4, for the Cu(II)/malonate system (R is CH_2) both $CH_3C(O)O^{-}$ and $CH_2(OH)C(O)O^{-}$ are expected as organic photoproducts; both compounds were formed during illumination (313 nm) of the Cu(II)/malonate system ($[Cu(II)]_T = 50$ μM, pH = 7.00, $[L]_T = 800$, 1700 μM), consistent with previous findings at 254 nm.[24] Flash photolysis of Cu(II)/malonate solutions forms an intermediate that was tentatively assigned as $[Cu^{I}(^{-}O(O)C-R^{\bullet})]^{0}$,[23,24] which is quenched by free malonate species,[23,24] thereby decreasing the Cu(I) quantum yield. This will be the subject of a future paper.

For Cu(II)/succinate (R is CH_2CH_2) and Cu(II)/maleate (R is CH=CH) systems, measured values of $\Phi_{Cu(I)}\epsilon_{Cu(II)} - \Phi_{Cu(I),in}\epsilon_{in}f_{in}$ at 313 nm are successfully quantified by eq 6. Moreover, the Cu(I) quantum yield was not affected by quenching by free succinate or maleate species, and we are not aware of any published effect of this type of quenching for these systems.

Still other factors can influence the Cu(I) quantum yield. The pK_a value of the protonated radical $^{\bullet}R-C(O)OH$ (e.g., pK_a < 3 for $HCO_2^{\bullet}$, p$K_a \approx 4.5-4.9$ for R is CH_2)[52,53] and the pH of the solution affect the speciation of $^{\bullet}R-C(O)OH/^{\bullet}R-C(O)O^{-}$. This pH-dependent radical speciation can also influence the Cu(I) quantum yield since, presumably, $^{\bullet}R-C(O)O^{-}$ is a better reductant of Cu(II) and $^{\bullet}R-C(O)OH$ is a better oxidant of Cu(I).

It is likely that for a given stoichiometry (e.g., CuL), some Cu(dicarboxylate)^0 complexes are primarily inner-sphere-type complexes, while other Cu(dicarboxylate)^0 complexes exhibit more outer-sphere coordination. The presence of one or more water molecules between Cu^{2+} and dicarboxylate^{2-} in an outer-sphere Cu(dicarboxylate)^0 complex must affect the efficiency of the photoinduced electron transfer, to form [$^{-}O(O)C-R-C(O)O^{\bullet}$ Cu(I)], and hence the Cu(I) quantum yield of the complex.

One measure of the degree of inner-sphere versus outer-sphere coordination of a complex is the stability constant for its formation. A larger stability constant, above a minimum outer-sphere value, indicates more inner-sphere-type coordination.[54] The stability constants for Cu(dicarboxylate)^0 complexes [$\log_{10}$ (β, M) (25 °C, $I = 0.10$ M, 1 atm)] are 4.85 for oxalate, 5.04 for malonate, 2.70 for succinate, 3.41 for maleate, 2.37 for glutarate, 2.3 for adipate, and 2.21 for pimelate.[41] The equilibrium constant for Cu(pimelate)^0 very likely represents the approximate minimum value for outer-sphere Cu(dicarboxylate)^0 complexes for these conditions. Based on this criteria, the Cu(dicarboxylate)^0 complexes studied here (oxalate, succinate, maleate) are primarily inner-sphere complexes. Therefore, their Cu(I) quantum yields should not exhibit significant variability due to differences in the degree of inner-sphere versus outer-sphere coordination. However, complexes of Cu(glutarate)^0, Cu(adipate)^0, and Cu(pimelate)^0 are likely to be primarily outer sphere, and their photoreactions will be the subject of the future paper.

The Cu(dicarboxylate)^0 complexes studied here could form five-member to seven-member rings. Dicarboxylate ligand structure also affects the lifetimes and rates of intramolecular electron transfer of Cu(dicarboxylate)^0 excited states, which influence the Cu(I) quantum yield. However, comparative information is not available from the literature on lifetimes of these Cu(II)/dicarboxylate excited states.

Photoreaction Rate Constants in Sunlight. The calculated apparent first-order rate constants for photoproduction of Cu(I) from the Cu(II)/dicarboxylate complexes in terrestrial sunlight (solar zenith angle = 30°), $j_{i\rightarrow Cu(I)}$ (s^{-1}), are 9.9×10^{-5} for Cu(oxalate)^0, 7.9×10^{-5} for Cu(oxalate)$_2^{2-}$, 2.4×10^{-5} for Cu(succinate)^0, and 2.2×10^{-6} for Cu(maleate)^0. Reduction of Cu(II) by photochemically formed $^{\bullet}O_2^{-}$ is an important source of Cu(I) in natural waters.[55-57] However, in this reaction (unlike photoreactions of Cu(II)) there is apparently no oxidation of the organic functional group/ligand responsible for coordination of Cu(II). Because the absorption spectra of the Cu(II)/dicarboxylate complexes studied here overlap the terrestrial solar spectrum (wavelength > 290 nm)[16] primarily in the ultraviolet-B region, sunlight photoreaction rate constants for these complexes could be highly sensitive to future changes (e.g., increases) in terrestrial solar ultraviolet-B irradiance.

Conclusions

In this study, a quantitative method that combines experimental measurements and the calculated equilibrium Cu(II) speciation is developed to determine molar absorptivities and Cu(I) quantum yields for different Cu(dicarboxylate)^0 complexes. This allows the effects of dicarboxylate ligand structure on the Cu(I) quantum yield to be compared between different inner-sphere Cu(II)/dicarboxylate complexes of the same stoichiometry.

The Cu(I) quantum yields of Cu(dicarboxylate)^0 follow the trend: Cu(oxalate)^0 > Cu(succinate)^0 ≫ Cu(maleate)^0, which is consistent with the expected trend in relative stability of the carbon-centered radicals derived from decarboxylation of the carboxylate radicals formed from the ligand-to-metal charge (electron) transfer.

Acknowledgment. This study was supported by the U.S. Office of Naval Research, Harbor Processes Program. A portion of this work was presented at the 210th national meeting of the American Chemical Society.

Supporting Information Available: Text, tables, and figures containing additional information about the molar absorptivities and the photochemistry of the Cu(II)/dicarboxylate systems studied here (14 pages). Ordering information is given on any current masthead page.

References and Notes

(1) Keith, L. H.; Telliard, W. A. *Environ. Sci. Technol.* **1979**, *13*, 416−423.
(2) Sunda, W. G.; Guillard, R. R. L. *J. Mar. Res.* **1976**, *34*, 511−529.
(3) Sunda, W. G.; Hanson, P. J. In *Chemical Modeling in Aqueous Systems*; Jenne, E. A., Ed.; Am. Chem. Soc. Symp. Ser. 93; 1979; Chapter 8.
(4) Sunda, W. G.; Huntsman, S. A. *Mar. Chem.* **1991**, *36*, 137−163.
(5) Moffett, J. W.; Zika, R. G. In *Photochemistry of Environmental Aquatic Systems*; Zika, R. G., Cooper, W. J., Eds.; Am. Chem. Soc. Symp. Ser. 327; 1987; Chapter 9.
(6) Sunda, W. G.; Gillespie, P. A. *J. Mar. Res.* **1979**, *37*, 761−777.
(7) Morel, F. M. M.; Hering, J. *Principles and Applications of Aquatic Chemistry*; Wiley: New York, 1993.
(8) Xue, H. B.; Sigg L. *Limnol. Oceanogr.* **1993,** *38*, 1200−1213.
(9) Mills, G. L.; Hanson, A. K., Jr.; Quinn, J. G.; Lammela, W. R.; Chasteen, N. D. *Mar. Chem.* **1982,** *11*, 355−377.
(10) Moffett, J. W.; Zika, R. G.; Brand, L. E. *Deep-Sea Res.* **1990,** *37*, 27−36.
(11) Donat, J. R.; Lao, K. A.; Bruland, K. W. *Anal. Chim. Acta* **1994,** *284*, 547−571.
(12) Azenha, M.; Vasconcelos, M. T.; Cabral, J. P. S. *Environ. Toxicol. Chem.* **1995**, *14*, 369−373.
(13) Langford, C. H.; Wingham, M.; Sarstri, V. S. *Environ. Sci. Technol.* **1973**, *7*, 820−822.
(14) Ferraudi, G.; Muralidharan, S. *Coord. Chem. Rev.* **1981**, *36*, 45−88.
(15) Hayase, K.; Zepp, R. G. *Environ. Sci. Technol.* **1991**, *25*, 1273−1279.
(16) Faust, B. C. In *Aquatic and Surface Photochemistry*; Helz, G. R., Zepp, R. G., Crosby, D. G., Eds.; CRC Press: Boca Raton, FL; 1994; Chapter 1.
(17) Thurman, E. M. *Organic Geochemistry of Natural Waters*; Martinus Nijhoff/Dr. W. Junk: Boston, 1985.
(18) Klug-Roth, D.; Rabani, J. *J. Phys. Chem.* **1976**, *80*, 588−591.
(19) Willix, R. L. S.; Garrison, W. M. *J. Phys. Chem.* **1965**, *69*, 1579−1583.
(20) Mailhot, G.; Andrianirinaharivelo, S. L.; Bolte, M. *J. Photochem. Photobiol. A: Chem.* **1995**, *87*, 31−36.
(21) Namasivayam, C.; Natarajan, P. *J. Polym. Sci.: Polym. Chem. Ed.* **1983**, *21*, 1371−1384.
(22) Natarajan, E.; Ramamurthy, P.; Natarajan, P. *Proc. Indian Acad. Sci. (Chem. Sci.)* **1990**, *102*, 319−328.
(23) Morimoto, J. Y.; DeGraff, B. A. *J. Phys. Chem.* **1972**, *76*, 1387−1388.
(24) Morimoto, J. Y.; DeGraff, B. A. *J. Phys. Chem.* **1975**, *79*, 326−331.
(25) Balzani, V.; Carassiti, V. *Photochemistry of Coordination Compounds*, Academic Press: London, 1970; p 270.
(26) Bideau, M.; Claudel, B.; Faure, L.; Kazouan, H. *J. Photochem. Photobiol. A: Chem.* **1994**, *84*, 57−67.
(27) Das, S.; Johnson, G. R. A. *J. C. S. Faraday I* **1980,** *76*, 1779−1789.
(28) Rao, S. F.; Choppin, G. R. *Inorg. Chem.* **1984**, *23*, 2351−2354.
(29) Chateauneuf, J.; Lusztyk, J.; Ingold, K. U. *J. Am. Chem. Soc.* **1988,** *110*, 2886−2893.
(30) Hilburn, J. W.; Pinock, J. A. *J. Am. Chem. Soc.* **1991,** *113*, 2683−2686.
(31) Korth, H. G.; Chateauneuf, J.; Lusztyk, J.; Ingold, K. U. *J. Org. Chem.* **1991,** *56*, 2405−2410.
(32) Budac, D.; Wan, P. *J. Photochem. Photobiol. A: Chem.* **1992,** *67*, 135−166.
(33) Morimoto, J. Y.; DeGraff, B. A. *J. Phys. Chem.* **1972,** *76*, 1387−1388.
(34) Vaudo, A. F.; Kantrowitz, E. R.; Hoffman, M. Z.; Papaconstantinou, E.; Endicott, J. F. *J. Am. Chem. Soc.* **1972,** *94*, 6655−6665.
(35) May, D. D.; Skell, P. S. *J. Am. Chem. Soc.* **1982,** *104*, 4500−4502.
(36) Mulazzani, Q. G.; D'Angelantonio, M.; Venturi, M.; Hoffman, M. Z.; Rodgers, M. A. J. *J. Phys. Chem.* **1986,** *90*, 5347−5352.
(37) Horvath, O.; Papp, S. *J. Chem. Educ.* **1988**, *65*, 1102−1105.
(38) Faust, B. C. *Environ. Sci. Technol.* **1996,** *30*, 1919−1922.
(39) Allison, J. D.; Brown, D. S.; Novo-Gradac, K. J. *MINTEQA2/PRODEFA2, A Geochemical Assessment Model for Environmental Systems: Version 3.0 (EPA/600/3- 91/021)*; U. S. Environmental Protect Agency, Athens, GA; 1991.
(40) Smith, A. E.; Martell, R. M. *Critical Stability Constants Vols.* 1−6; Plenum: NY (1976−1989).
(41) Smith, A. E.; Martell, R. M.; Motekaitis, R. J. *NIST Critically Selected Stability Constants of Metal Complexes Database*, ver. 4.0, NIST Standard Reference Datatbase 46, 1995.
(42) Sase, E. G.; Jahagirdar, D. V. *J. Inorg. Nucl. Chem.* **1975,** *37*, 985−989.
(43) Stumm, W.; Morgan, J. J. *Aquatic Chemistry*; Wiley: New York, 1996; p 103.
(44) Margerum, D. W.; Cayley, G. R.; Weatherburn, D. C.; Pagenkopf, G. K. In *Coordination Chemistry*; Martell, A. E., Ed.; ACS Monograph 174; American Chemical Society: Washington, DC, 1978; Vol. 2, pp 1−220.
(45) Anastasio, C.; Faust, B. C.; Allen, J. M. *J. Geophys. Res.* **1994**, *99*, 8231−8248.
(46) Blair, D.; Diehl, H. *Talanta* **1961**, *7*, 163−174.
(47) Moffett, J. W.; Zika, R. G.; Petasne, R. G. *Anal. Chim. Acta* **1985**, *175*, 171−179.
(48) Peterson, J. T. Calculated Actinic Fluxes (290−700 nm) for Air Pollution Photochemistry Applications, EPA-600/4−76−025, 1976, 54 pp.
(49) Faust, B. C.; Powell, K.; Rao, C. J.; Anastasio, C. *Atmos. Environ.* **1997,** *31*, 497−510.
(50) Davis, D. D.; Stevenson, K. L.; Davis, C. R. *J. Am. Chem. Soc.* **1978**, *100*, 5344−5349.
(51) Ross, A. B.; Neta, P. Rate Constants for Reactions of Aliphatic Carbon-Centered Radicals in Aqueous Solution, NSRDS−NBS70, 1982, 96 pp.
(52) Neta, P.; Simic, M.; Hayon E. *J. Phys. Chem.* **1969,** *73*, 4207−4213.
(53) Hoffman, M. Z.; Hayon, E. *J. Phys. Chem.* **1973,** *77*, 990−996.
(54) Hancock, R. D.; Martell, A. E. *Chem. Rev.* **1989,** *89*, 1875−1914.
(55) Micinski, E.; Ball, L. A., Zafiriou, O. C. *J. Geophys. Res.* **1993,** *98*, 2299−2306.
(56) Voelker, B. M.; Sedlak, D. L. *Marine Chem.* **1995,** *50*, 93−102.
(57) Voelker, B. M.; Zafiriou, O. C.; Sedlak, D. L *Prepr. Papers Am. Chem. Soc. Meeting (Environ. Chem. Div.)* **1995,** *35*, 451−454.